Available online at www.sciencedirect.com
ScienceDirect
Mendeleev Commun., 2023, **33**, 285–286

Mendeleev Communications

Magnetic sorbent modified by humate for the extraction of alkylphenols, bisphenol A and estradiol

Alexander S. Gubin,* Pavel T. Sukhanov and Aleksei A. Kushnir

Voronezh State University of Engineering Technologies, 394036 Voronezh, Russian Federation.
E-mail: goubinne@mail.ru

DOI: 10.1016/j.mencom.2023.02.044

A sorbent has been synthesized from magnetite nanoparticles and a humic acid extracted from sapropel. The sizes of the sorbent nanoparticles and their magnetic core are 218–302 and 14 nm, respectively, the saturation magnetization is 35 emu g^{-1}. The sorbent provides 87–95% recoveries of alkylphenols, bisphenol A and estradiol with enrichment factors of 1550–1815.

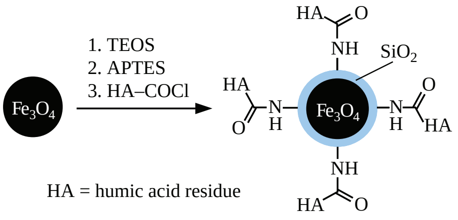

Keywords: alkylphenols, bisphenol A, estradiol, magnetic nanosorbent, humic acid.

Alkylphenols, bisphenols (BPLs) and estradiol (17β-estradiol, E2) represent endocrine disruptors (EDs),[1] which after penetration into water bodies can adversely affect the aquatic biota resulting in its feminization. BPLs are related to the production of plastics[2] and enter into the aquatic media together with industrial wastes. Nonylphenols (NLPs) are used as household surfactants, while their esters represent commercial-scale synthetic products.[3] E2 is a female sex hormone excreted by urinary way into natural waters together with sewage effluents.[4] 4-Octylphenyl (4-OP), 4-nonylphenol (4-NLP), bisphenol A (BPA) and E2 are poorly soluble in water and have an affinity to hydrophobic matrices.[5] Their content in aquatic media is typically less than 0.1 μg dm^{-3}.[6] It is reasonable to estimate the contamination level of water bodies from the analysis of bottom sediments, where lipids, petroleum products as well as other hydrophobic components are present.[7] For different areas around the world, the EDs concentration in bottom sediments varies from 2 to 1000 μg kg^{-1}.[8–10]

Humic acids (HAs) represents known sorbents for organic substances[11] including phenols,[12,13] but their direct application is restricted by inappropriate desorption time and partial solubility in most organic solvents, that hampers their reuse. In the last two decades, methods for efficient immobilization of HAs have been developed resulting in promising sorbents and/or chromatographic phases.[14,15] However, due to their instability these materials can hardly be applied for the analysis of aqueous media.

The aim of this work was to synthesize new HA-based sorbents and estimate whether magnetite nanoparticles (NPs) modified by humate could be applied for the concentration of EDs from nonaqueous media for the following GC–MS determination.

We used the described methods for preparation of Fe_3O_4 NPs and the extraction of HA from sapropel (for details, see Online Supplementary Materials).[12,13] The synthesis of HA-modified magnetite NPs is outlined in Scheme 1.[†]

According to SEM data, the size of the $Fe_3O_4@SiO_2$–HA NPs was 218–302 nm [Figures 1(*a*) and S1, see Online Supplementary Materials], their saturation magnetization was 35 emu g^{-1} [Figure 1(*b*)], while for the starting magnetite NPs it was 60 emu g^{-1}. The powder XRD pattern of Fe_3O_4 (Figure S2) contains the peaks of magnetite (2θ = 30.38, 35.58, 44.14, 53.48, 57.08 and 62.66°) corresponding to the (2 1 1), (3 1 1), (4 0 0), (4 2 2), (5 1 1) and (4 4 0) intensities.[12] The diffraction pattern of $Fe_3O_4@SiO_2$–HA contains wide peaks at 2θ = 20–29°, which are related to amorphous silica surrounding the Fe_3O_4 NPs. The

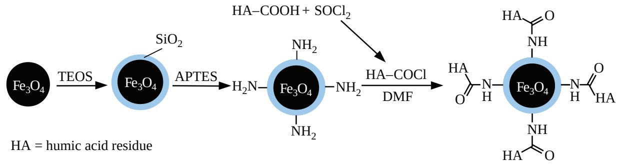

Scheme 1 Synthesis of the $Fe_3O_4@SiO_2$–HA sorbent.

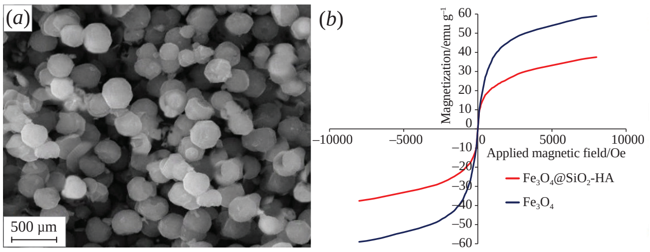

Figure 1 (*a*) SEM image of $Fe_3O_4@SiO_2$–HA, (*b*) magnetization curves for Fe_3O_4 and $Fe_3O_4@SiO_2$–HA.

[†] Fe_3O_4 NPs were stabilized by sodium citrate. Tetraethyl orthosilicate (8 ml) was added to the stabilized suspension (5 ml), then aq. ammonia was added until pH 9.0. The mixture was stirred for 6 h, washed with distilled water and ethanol, then dried at 40–45 °C for 12 h *in vacuo* resulting in silica-coated Fe_3O_4 particles ($Fe_3O_4@SiO_2$). To modify their surface with NH_2 groups, the particles were reacted with (3-aminopropyl)-triethoxysilane (1% solution in isopropanol) for 4 h under continuous stirring. The resulting $Fe_3O_4@SiO_2$–NH_2 particles were washed with toluene and acetone. Thionyl chloride (25 ml) was added to HA (1 g) extracted earlier from sapropel and stirred at 300 rpm for 16 h, then the mixture was evaporated to dryness. The resulting humyl chloride (1 g) was added to the $Fe_3O_4@SiO_2$–NH_2 particles (2 g) in DMF (30 ml) and the mixture was stirred at 60 °C for 12 h. The humate-modified Fe_3O_4 NPs ($Fe_3O_4@SiO_2$–HA) were retrieved from the reaction mixture with a magnet and washed with dichloroethane and acetone.

XRD pattern agrees with the diffraction databases and known data typical of the cubic inverse spinel structure of magnetite NPs.

The FT-IR spectrum of Fe_3O_4@SiO_2–HA reveals bands at *ca.* 804, 958 and 1077 cm^{-1} corresponding to symmetric vibrations of Si–O bonds, vibrations typical of the N–H (1412, 3396 cm^{-1}) and Fe–O (570 cm^{-1})[13] bonds as well as the CH_2 and CH_3 groups (2850–2970 cm^{-1})[12] (Figure S3). The IR spectrum also contains bands of HA extracted from sapropel, namely, 1032, 1210, 1600, 1624 and 1706 cm^{-1}. For the Fe_3O_4@SiO_2 and Fe_3O_4@SiO_2–HA materials, respectively, the specific surface area was 238 and 194 $m^2\,g^{-1}$, the mean pore size was equal to 12 and 7 nm, while the specific pore surface area was 1.09 and 0.81 $cm^3\,g^{-1}$. Elemental analysis revealed the presence of oxygen, iron, nitrogen, silicon, carbon and chlorine in the synthesized sorbent (Figure S4), chlorine presumably originated from an unreacted reagent impurity.

Preconcentration procedure was carried out using the online magnetic solid phase extraction (MSPE) scheme.[16] Fe_3O_4@SiO_2–HA was placed in a borosilicate glass tube with a diameter of 2 mm. Magnets were arranged on two sides of the tube (Figure S5). The sorbent (0.05 g) was held in the tube due to supermagnetic properties and occupied its entire cross section. Then a solution of 4-OP, 4-NLP, BPA or E2 in hexane was passed through the tube. Equilibrium concentrations of the analytes before and after their sorption were determined by GC–MS (Figure S6). Desorption was carried out using methanol (1 ml), which was then evaporated to a volume of 0.1 ml in the stream of nitrogen. Upon passing through the cartridge, the best interaction with Fe_3O_4@SiO_2–HA was achieved in part by filtration through the sorbent pad. On the other hand, the sorbent held by the magnet had no dense packing, so neither its compaction nor near-wall effects were observed.

The recoveries of analytes varied from 87% for 4-OP to 95% for E2 (Table 1). The sorption isotherms were satisfactorily described using the Langmuir equation. The sorption capacity of Fe_3O_4@SiO_2–HA varied from 740 to 1022 $mg\,g^{-1}$. The extraction efficacy was estimated from the enrichment factor (EF) calculated using the following equation:

$$\mathrm{EF} = C_\mathrm{E}/C_0, \tag{1}$$

where C_E was the concentration of an analyte after desorption with methanol and C_0 represented its initial concentration.

Then the Fe_3O_4@SiO_2–HA sorbent was tested for concentrating EDs from bottom sediments. A model sediment sample was collected in the background area of the water basin with negligible human impact. A known amount of 4-OP, 4-NLP, BPA or E2 was used for the sorption (for details of the analysis, see Figure S7). The limit of detection for EDs in the model samples was 0.9–1.8 ng kg^{-1} dry wt (Table S1). The data for the real ED-contaminated sample of bottom sediments are gathered in Table S2. As follows from the cumulated data of Table S3, the enrichment factor and the sorption capacity (see Table 1) for the method developed here exceed those of known solid phase extraction methods with magnetic sorbents.[17–22]

Table 1 Parameters of sorption at pH 3 and the Fe_3O_4@SiO_2–HA sorbent amount of 5.0 g dm^{-3}.

ED	EF	Recovery (%)	Sorption capacity/ mg g^{-1}	Langmuir equation		Freundlich equation		
				K_L	r^2	n	K_F	r^2
4-OP	1550	87	740	0.0258	0.991	0.6353	20.510	0.783
4-NLP	1618	89	809	0.0316	0.982	0.6222	6.576	0.925
BPA	1782	92	895	0.0433	0.985	0.6850	38.115	0.933
E2	1815	95	1022	0.0217	0.984	0.5821	34.518	0.857

Online Supplementary Materials

Supplementary data associated with this article can be found in the online version at doi: 10.1016/j.mencom.2023.02.044.

References

1 E. Diamanti-Kandarakis, J.-P. Bourguignon, L. C. Giudice, R. Hauser, G. S. Prins, A. M. Soto, R. T. Zoeller and A. C. Gore, *Endocr. Rev.*, 2009, **30**, 293.

2 M. Fürhacker, S. Scharf and H. Weber, *Chemosphere*, 2000, **41**, 751.

3 T. B. Chokwe, J. O. Okonkwo and L. L. Sibali, *Water SA*, 2017, **43**, 529.

4 M. Forghani, G. Sadeghi and M. Peyda, *Int. J. Epidemiol. Res.*, 2018, **5**, 151.

5 S. Mortazavi, A. R. Bakhtiari, A. E. Sari, N. Bahramifar and F. Rahbarizade, *Mar. Pollut. Bull.*, 2012, **64**, 1067.

6 C. Pironti, M. Ricciardi, A. Proto, P. M. Bianco, L. Montano and O. Motta, *Water*, 2021, **13**, 1347.

7 Z. Yang, K. Shah, S. Laforest, C. Courtemanche, W. Durand, P. Lambert, B. P. Hollebone, C. E. Brown, M. Goldthorp, K. Watson, C. Yang, D. Dey and V. Beaulac, *Mar. Pollut. Bull.*, 2021, **173**, 113037.

8 W. Ruczyńska, J. Szlinder-Richert and A. Drgas, *Environ. Sci.: Processes Impacts*, 2016, **18**, 1193.

9 A. Filipkowska, L. Lubecki, M. Szymczak-Żyła, T. M. Ciesielski, B. M. Jenssen, M. V. Ardelan, H. Mazur-Marzec, G. D. Breedveld, A. M. P. Oen, A. Zamojska and G. Kowalewska, *Mar. Pollut. Bull.*, 2018, **133**, 328.

10 D. Liu, S. Wu, H. Xu, Q. Zhang, S. Zhang, L. Shi, C. Yao, Y. Liu and J. Cheng, *Ecotoxicol. Environ. Saf.*, 2017, **140**, 222.

11 S. Chianese, A. Fenti, P. Iovino, D. Musmarra and S. Salvestrini, *Molecules*, 2020, **25**, 918.

12 A. Gubin, P. Sukhanov, A. Kushnir, K. Shikhaliev, M. Potapov and E. Kovaleva, *Environ. Nanotechnol., Monit. Manage.*, 2022, **17**, 100652.

13 A. S. Gubin, P. T. Sukhanov and A. A. Kushnir, *Moscow Univ. Chem. Bull.*, 2019, **74**, 257 (*Vestn. Mosk. Univ., Ser. 2: Khim.*, 2019, 338).

14 D. Luo, Q.-W. Yu, H.-R. Yin and Y.-Q. Feng, *Anal. Chim. Acta*, 2007, **588**, 261.

15 N.-Z. Zhou, P. Liu, X.-C. Su, Y.-H. Liao, N.-S. Lei, Y.-H. Liang, S.-H. Zhou, W.-S. Lin, J. Chen, Y.-Q. Feng and Y. Tang, *Anal. Chim. Acta*, 2017, **970**, 38.

16 G. Giakisikli and A. N. Anthemidis, *Talanta*, 2013, **110**, 229.

17 Q. Zhou, M. Lei, J. Li, K. Zhao and Y. Liu, *Sep. Purif. Technol.*, 2017, **182**, 78.

18 S. Han, X. Li, Y. Wang and S. Chen, *Chem. Eng. J.*, 2015, **271**, 87.

19 W. Rao, R. Cai, Y. Yin, F. Long and Z. Zhang, *Talanta*, 2014, **128**, 170.

20 Z.-D. Du, Y.-Y. Cui, C.-X. Yang and X.-P. Yan, *Talanta*, 2020, **206**, 120179.

21 A. Karrat and A. Amine, *Microchem. J.*, 2021, **168**, 106496.

22 F. N. Ferreira, A. P. Benevides, D. V. Cesar, A. S. Luna and J. S. de Gois, *Microchem. J.*, 2020, **157**, 104947.

Received: 24th August 2022; Com. 22/6987